Desalination and Water Treatment
www.deswater.com

doi: 10.5004/dwt.2019.24059

155 (2019) 311–320
July

Removal of fluoride from water using thermally treated dolomite and optimization of experimental conditions using response surface methodology

Mun-Ju Kim[a], Seung-Hee Hong[a], Jae-In Lee[a], Chang-Gu Lee[b], Seong-Jik Park[a,*]

[a]*Department of Bioresources and Rural System Engineering, Hankyong National University, Anseong, South Korea, Tel. +82-31-670-5131; Fax: +82-31-670-5139; email: parkseongjik@hknu.ac.kr (S.-J. Park)*
[b]*Department of Environmental and Safety Engineering, Ajou University, Suwon, South Korea, email: changgu@ajou.ac.kr*

Received 4 October 2018; Accepted 28 February 2019

ABSTRACT

This study was performed to identify an economical but highly effective adsorbent for the removal of fluoride. Dolomite was thermally treated to improve its adsorption capacity for fluoride; dolomite thermally treated at 800°C (DTT-800) was superior to that treated at other temperatures. The maximum fluoride adsorption capacity of DTT-800 was 163.7 mg g^{-1}, which was superior to that of other adsorbents reported in the literature. Fluoride adsorption onto DTT-800 was characterized by chemisorption, multi-layer adsorption, and an endothermic reaction. Response surface methodology was employed to investigate the influence pH, ionic strength, reaction temperature, and time on fluoride adsorption; these parameters were optimized to maximize the adsorption process. pH and ionic strength had a negative effect, while reaction temperature and time had a positive effect on fluoride adsorption. The influence of all four parameters was significant (p <0.001). Highest fluoride adsorption (165.91 mg g^{-1}), was obtained under the following conditions: pH 4.57, ionic strength 7.45 mM, temperature 28.30°C, and contact time 58.33 h. This study demonstrated that DTT-800 is a low-cost, natural, and abundant material for the removal of fluoride from aqueous solutions.

Keywords: Fluoride; Thermal treatment; Dolomite; Adsorption; Response surface methodology; Optimization

1. Introduction

Groundwater can be contaminated with high concentrations of fluoride through natural and anthropogenic activities [1]. Fluoride is generally released into the groundwater by the slow dissolution of fluoride-rich rocks. Industrial activities, such as glass and ceramic production, semiconductor manufacturing, electroplating, and coal-fired power stations, also discharge wastewater containing high fluoride concentrations [2]. A small amount (0.5–1.0 mg L^{-1}) of fluoride is beneficial for bone and teeth health, but concentrations higher than 1.5 mg L^{-1} can cause dental or skeletal fluorosis [3,4]. High concentrations of fluoride in groundwater have been reported from Southeastern Africa, the United States, the Middle East, South America, and Asian countries, especially China and India [1].

Fluoride removal from water is achieved using many technologies, such as membrane techniques, electrocoagulation-flotation, electrodialysis, ion exchange, coagulation/precipitation, and adsorption [1]. Among these, coagulation/precipitation and adsorption are the most widely used. Coagulation/precipitation requires large quantities of chemicals, generating a corresponding amount of sludge that must be disposed [5]. Aluminum salt is commonly used as a coagulant for fluoride removal, but aluminum concentration over 0.2 mg L^{-1} in drinking water can cause serious health problems, including dementia [6]. Adsorptive filtration has several advantages, such as low cost, low energy consumption, and ease of operation [7]. The practical applicability of adsorption depends on the efficiency, cost performance, and regeneration of the adsorbent materials. To meet these criteria, many research

* Corresponding author.

groups have focused their studies on low-cost naturally occurring adsorbents, such as activated carbon from plant materials, bone-char powder, fly ash, rice husk, gibbsite, kaolinite, tea ash powder, and clay minerals [2,8]. Although, being economically advantageous, their fluoride removal efficiency is not usually high. Some of the artificially synthesized materials, such as Fe–Al–Ce trimetal oxide [9], Al–Ce hybrid adsorbent [10], and nano-magnesia [11], have high adsorption capacity, but the cost of their synthesis is not economical for treating large quantities of water. Research is underway to obtain economical as well as highly effective adsorbents for fluoride removal.

Dolomite ($CaMg(CO_3)_2$) is a common rock-forming mineral found in sedimentary beds, metamorphic marbles, hydrothermal veins, and replacement deposits [12]. It consists mostly of magnesium oxide (MgO), calcium oxide (CaO), and carbon dioxide (CO_2). CaO easily produces precipitates and serves as a pH neutralizing agent, and thus is widely used in water treatment [13].

To investigate the adsorption characteristics of the adsorbents, batch and column experiments have been performed using conventional methods that involve variations in a single parameter while the others are kept constant. This method requires many experimental runs, requiring significant investment of time and chemicals, to determine the optimal conditions for contaminant removal. Using the conventional method, it is also difficult to investigate the effects of interactions between the process parameters [14]. These limitations can be overcome by applying a well-known statistical method, response surface methodology (RSM). RSM involves the simultaneous variation in many factors over a set of experimental runs and enables the elucidation of optimized conditions and evaluation of the relative significance of several factors, even in the presence of complex interactions [15,16]. A statistically designed experimental plan enables the optimization and analysis of experimental factors with a small number of experimental runs. Full factorial design, central composite design, and Box-Behnken design are the most widely used types of RSM. The Box-Behnken design has fewer design points than other designs, and requires less experimental data to operate with the same number of parameters [15,16].

In this study, we assessed the feasibility of dolomite for the removal of fluoride from aqueous solution. Thermally treated dolomite (TTD) was used to enhance its adsorption capacity for fluoride. The physical and chemical properties and adsorption capacities of dolomite treated at different temperatures were investigated. Dolomite thermally treated at 800°C (DTT-800) was used for further investigations, including kinetic, equilibrium, and thermodynamic studies. We also suggested the application of RSM to analyze the data obtained from batch experiments. This study applied the Box-Behnken design to optimize the experiments and elucidate the effect of parameters and their interactions on fluoride removal by DTT-800. The investigated parameters included solution pH, ionic strength, temperature, and reaction time.

2. Materials and methods

2.1. Thermal treatment of dolomite and characterization of thermally treated dolomite

The experiment was performed with natural dolomite supplied by Rexem Co., Korea. The particle size of the dolomite was 9 μm. The dolomite was thermally treated using a tube furnace with a horizontal quartz glass tube at 100, 300°C, 500°C, 700°C, 800°C, and 900°C (DTT-100, DTT-300, DTT-500, DTT-700, DTT-800, and DTT-900, respectively) for 4 h under anoxic conditions. The heating rate was set to 8°C min^{-1}. TTD was stored in desiccators before use.

The physical and chemical properties of TTD were investigated using various methods. A field emission scanning electron microscope (FE-SEM; S-4700, Hitachi, Japan) was used to investigate the surface morphologies of the dolomite. The specimens of dolomite were observed at 5,000× magnification at an accelerating voltage of 5 kV. Before imaging, all samples were coated with gold at 30 mA for 120 s to minimize the charging effect. The mineralogical structures of the dolomite were investigated via X-ray diffraction (XRD) patterns (Rigaku Co., Japan) with CuKα radiation at a fixed power of 40 kV and 30 mA. The diffraction data were collected over a 2θ range between 3° and 90° at a scanning rate of 2.0° min^{-1}. N_2 adsorption-desorption experiments were performed to measure the specific surface area of the dolomite using a surface area analyzer (Quadrasorb SI, Quantachrome Instrument, USA). From the N_2 adsorption-desorption isotherms, the specific surface area was determined via Brunauer-Emmett-Teller analysis. The chemical composition of the dolomite was also analyzed using an X-ray fluorescence spectrometer (XRF-1700, Shimadzu, Japan).

2.2. Adsorption experiment

The fluoride removal efficiency of TTD was evaluated under batch conditions. First, 0.1 g of dolomite was reacted with 30 mL of 100 mg L^{-1} fluoride solution in a 50 mL Falcon tube for 24 h. The tubes were agitated in a shaking incubator (SJ-808SF, Sejong Scientific Co., Korea) at 100 rpm. After the adsorption reaction, the fluoride solution was separated from the adsorbent using a syringe filter (0.45 μm, Whatman, USA). Then, the fluoride concentration was analyzed using ion chromatography (DX-120, Dionex, USA). A standard 1,000 mg L^{-1} fluoride solution was obtained by dissolving sodium fluoride (NaF, Sigma-Aldrich, USA), and the fluoride solution was prepared by diluting the standard solution with deionized water. All batch experimental conditions were identical to those described above unless otherwise stated. The experiments were performed in triplicate.

Kinetic, equilibrium, and thermodynamic adsorption experiments were performed with DTT-800, which was found to be the most efficient dolomite for fluoride removal, to investigate the fundamental characteristics of fluoride adsorption. The kinetic adsorption experiments were performed by reacting 0.1 g of DTT-800 with 30 mL of 300 mg L^{-1} and 1,000 mg L^{-1} fluoride solution, and the fluoride solution was sampled 0.25, 0.5, 1, 6, 24, 72, 120, 144, and 168 h after reaction initiation. In the equilibrium isotherm experiments, the initial concentrations of the fluoride solutions were set at 5, 10, 50, 100, 300, 500, 700, 1,000, 1,500, and 2,000 mg L^{-1}, and the solution samples were sampled after 72 h. The thermodynamic adsorption experiments were performed by reacting 0.1 g of DTT-800 with 30 mL of 1,000 mg L^{-1} fluoride solution for 72 h under different reaction temperatures of 15°C, 25°C, and 35°C.

Four parameters, namely pH, ionic strength, reaction temperature, and reaction time, were investigated to assess

their influence on the removal of fluoride by DTT-800. Batch experiments were performed by reacting 0.1 g of DTT-800 with 30 mL of 1,000 mg L^{-1} fluoride solution under different experimental conditions. The desired pH (4, 6, and 8) was adjusted using 1 M HCl and 1 M NaOH solutions. The ionic strength of the solution was adjusted to 0, 10, and 20 mM using KCl. The detailed experimental design is explained in Section 2.4.

The removal of fluoride by DTT-800 after regeneration was investigated. After the adsorption experiment with 0.1 g of DTT-800 and 30 mL of 1,000 mg L^{-1} fluoride solution, the separated DTT-800 was agitated in 30 mL of deionized water to desorb the fluoride from the DTT-800. Additional adsorption tests were conducted using the same procedure described in this section. The DTT-800 was regenerated three times in this adsorption experiment.

2.3. Data analysis

The kinetic data were analyzed using the following pseudo-first-order and pseudo-second-order models:

$$q_t = q_e\left(1 - e^{-k_1 t}\right) \tag{1}$$

$$q_t = \frac{k_2 q_e^2 t}{1 + k_2 q_e t} \tag{2}$$

where q_t is the amount of fluoride removed at time t (mg F g^{-1}), q_e is the amount of fluoride removed at equilibrium (mg F g^{-1}), k_1 is the pseudo-first-order rate constant (1/h), and k_2 is the pseudo-second-order rate constant (g (mg F·h)$^{-1}$).

The equilibrium data were analyzed using the Langmuir (Eq. (3)) and Freundlich (Eq. (4)) models as follows:

$$q_e = \frac{Q_m K_L C}{1 + K_L C} \tag{3}$$

$$q_e = K_F C_e^{\frac{1}{n}} \tag{4}$$

where C is the concentration of fluoride in the aqueous solution at equilibrium (mg F g^{-1}), K_L is the Langmuir constant related to the binding energy (L mg^{-1} F), Q_m is the maximum amount of fluoride removed per unit mass of dolomite (mg F g^{-1}), K_F is the distribution coefficient ((mg F g^{-1})·(L mg^{-1} F)$^{1/n}$), and n is the Freundlich constant.

The thermodynamic properties of the experimental results were analyzed using the following equations:

$$\Delta G° = \Delta H° - T\Delta S° \tag{5}$$

$$\Delta G° = -RT\ln K_e \tag{6}$$

$$\ln K_e = \frac{\Delta S°}{R} - \frac{\Delta H°}{RT} \tag{7}$$

$$K_e = \frac{\alpha q_e}{C_e} \tag{8}$$

where $\Delta G°$ is the change in Gibbs free energy (kJ mol^{-1}), $\Delta S°$ is the change in entropy (J (K·mol)$^{-1}$), $\Delta H°$ is the change in enthalpy (kJ mol^{-1}), K_e is the equilibrium constant (–), and α is the amount of adsorbent (g L^{-1}).

2.4. Response surface methodology study

A Box-Behnken model in the RSM study was used to optimize the experimental conditions for fluoride removal using dolomite. Four independent variables, i.e., solution pH (4–8), ionic strength (0–20 mM), temperature (15°C–35°C), and reaction time (36–72 h), were selected. Two chemical parameters and two physical parameters that might influence fluoride removal using dolomite were selected. Overall, 29 sets of treatment combinations were analyzed using Design Expert statistical software (version 7.0.0, Stat-Ease Inc., Minneapolis, Minnesota, USA). A quadratic model was generated from the experimental data, which was also used for the analysis of variance (ANOVA) test to determine the significance of the obtained model. The highest order polynomial model that was not aliased and had a significant additional term was recommended by the statistical software. A quadratic model was generated from the data according to the following equation:

$$\begin{aligned} Y_A = {} & a_0 + a_1X_1 + a_2X_2 + a_3X_3 + a_4X_4 + a_{12}X_1X_2 \\ & + a_{13}X_1X_3 + a_{14}X_1X_4 + a_{23}X_2X_3 + a_{24}X_2X_4 \\ & + a_{34}X_3X_4 + a_{11}X_1^2 + a_{22}X_2^2 + a_{33}X_3^2 + a_{44}X_4^2 \end{aligned} \tag{9}$$

where Y_A is the predicted response of the amount of fluoride adsorbed onto a unit mass of DTT-800 (mg g^{-1}), x_i is the variables, and a_i is the model coefficient parameters. Subscripts 1, 2, 3, and 4 refer to pH, ionic strength, temperature, and reaction time, respectively. The design of this experiment included the dependent variables or responses shown in Table 1. To analyze the goodness-of-fit of the model, the regression coefficients (R^2), lack-of-fit, and adjusted and predicted R^2 values were also evaluated.

3. Results and discussion

3.1. Fluoride removal and characterization of thermally treated dolomite

TTD samples were characterized on the basis of surface morphology, specific surface area, pore volume, crystalline

Table 1
Factors and their levels for the Box-Behnken design

Variables	Symbol	Coded factor level		
		–1	0	1
pH	X_1	4	6	8
Ionic strength (mM)	X_2	0	10	20
Temperature (°C)	X_3	15	25	35
Reaction time (h)	X_4	36	54	72

structure, and chemical composition. The surface morphologies of the dolomite obtained using FE-SEM is shown in Fig. 1. As the temperature increased, the fragments on the surface of TTD became larger, and a rougher surface was formed. Thermal temperature increase from 500°C to 800°C, caused the specific surface area to increase from 2.71 to 11.14 $m^2 g^{-1}$ and pore volume from 0.01 to 0.08 $cm^3 g^{-1}$, respectively. The increase these parameters upon calcination could have been due to the release of CO_2 [17]. The specific surface area and pore volume of DTT-900 were less than those of DTT-800. This decrease in pore volume by thermal treatment could have been due to the formation of a slag from impurities, such as silica, potassium oxide, sodium oxide, and alumina, in the dolomite [18]. As shown in Fig. 2, the XRD patterns of untreated dolomite, DTT-100, DTT-300, and DTT-500 presented peaks corresponding to the structure of dolomite ($CaMg(CO_3)_2$), quartz (SiO_2), and calcium carbonate ($CaCO_3$). However, the peak intensity of dolomite significantly decreased at 700°C and disappeared at 800°C. In place of the dolomite peak, a periclase (MgO) peak appeared in the XRD pattern of DTT-800 and DTT-900. The present results were in good agreement with the theory of dolomite decomposition [17]; at temperatures 600°C–800°C, dolomite dissociates and magnesium carbonate decomposes and between 740°C and 880°C, $CaCO_3$ decomposes. The XRF results in Table 2 show that the weight percentage of CaO, MgO, SiO_2, and Al_2O_3 in dolomite increased as the thermal temperature increased. The increase in the weight percentage of inorganic substituents, such as CaO and MgO, could have been due to the total weight loss by the release of CO_2 (decarbonation) from the dolomite [18].

The treatment of fluoride adsorption onto dolomite at different temperatures is shown in Fig. 3. The amount of fluoride adsorbed onto the untreated dolomite was 3.45 mg g^{-1}, while that adsorbed onto DTT-100, DTT-300, and DTT-500 was 3.57, 3.62, and 3.86 mg g^{-1}, respectively, thereby showing an insignificant difference with that of untreated dolomite. For DTT-800°C, fluorine adsorption removal percentage increased to 29.49 mg g^{-1} and 98.3%, respectively, indicating that almost all fluoride in aqueous solution was removed by DTT-800. The observed results could have been due to the elution of Ca^{2+} ions from the decomposed dolomite at high temperature. Eluted Ca^{2+} ions reacted with the fluoride in aqueous solution and formed an insoluble precipitate (CaF_2; K_{sp} at 25°C = 3.45×10^{-11}). The elution of Ca^{2+} from thermally treated Ca-rich adsorbents, such as attapulgite and crushed concrete fines, has also been observed [19–21]. However, DTT-900 adsorbed less fluorine than DTT-800, even though the temperature and applied energy were higher. Higher fluoride adsorption capacity of DTT-800 could have been due to its larger specific surface area and pore volume providing larger sites for fluoride adsorption. Karaca et al. [22] also observed a reduction in the phosphate adsorption capacity of dolomite with increasing calcination temperature, and reported that this reduction was due to changes in the structure and pore size distribution of dolomite. As DTT-800 showed greatest fluoride adsorption, it was implemented for further experiments.

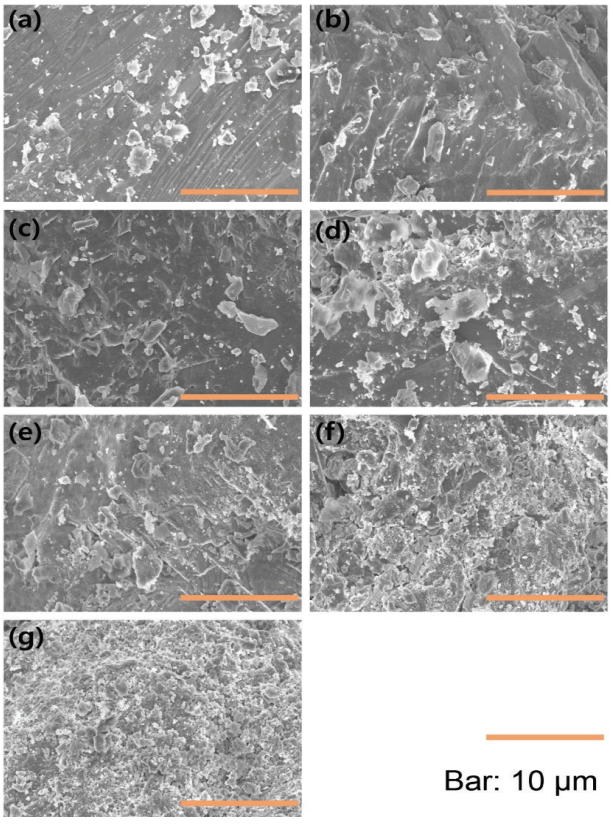

Fig. 1. Field emission scanning electron microscope images of thermally treated dolomite: (a) untreated, (b) 100°C, (c) 300°C, (d) 500°C, (e) 700°C, (f) 800°C, and (g) 900°C. Magnification: 5,000×.

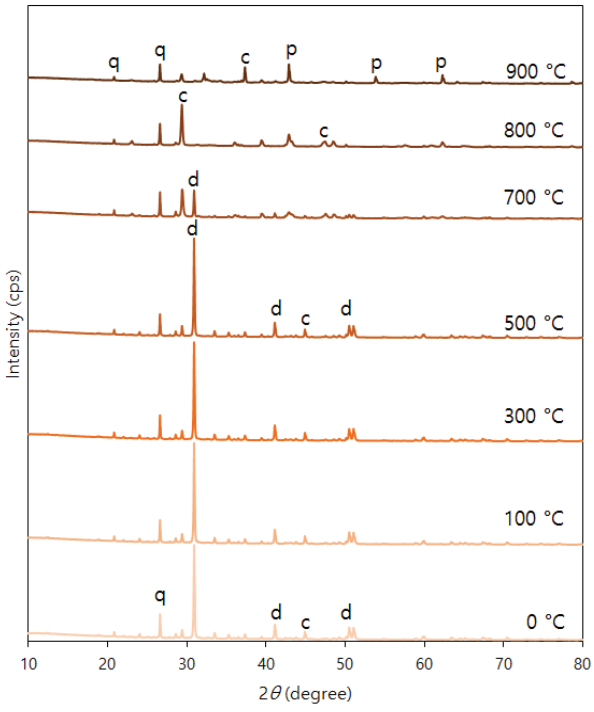

Fig. 2. X-ray diffraction results of dolomite treated at different temperatures (untreated, 100°C, 300°C, 500°C, 700°C, 800°C, and 900°C) (d: dolomite; q: quartz; c: calcite; p: periclase).

Table 2
Chemical and physical properties of thermally treated dolomite

Thermal temperature			Untreated	100°C	300°C	500°C	700°C	800°C	900°C
Physical properties	Surface area ($m^2 g^{-1}$)		2.88	2.29	2.40	2.71	5.70	11.14	8.41
	Pore volume ($cm^3 g^{-1}$)		0.01	0.01	0.01	0.01	0.05	0.08	0.05
	Pore size (nm)		20.15	10.82	14.81	10.32	35.75	30.49	25.63
Chemical properties	pH		9.44	9.68	8.84	10.20	10.27	11.57	12.46
	XRF	CaO	37.03	37.58	37.20	37.59	39.06	40.02	42.37
	result	MgO	19.12	18.75	17.95	19.16	21.60	23.61	28.23
	(%)	SiO_2	16.68	15.22	14.72	15.30	16.85	16.06	19.11
		Al_2O_3	1.84	1.64	1.56	1.65	1.84	1.74	2.47
		Fe_2O_3	1.46	1.50	1.55	1.55	1.51	1.52	2.08
		BaO	1.12	0.89	1.04	0.93	1.08	1.07	1.10

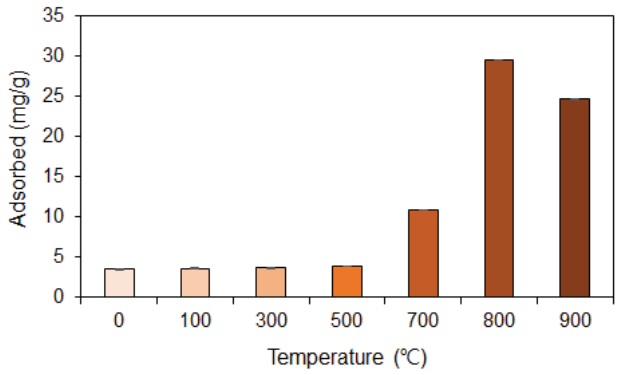

Fig. 3. Fluoride removal by dolomite treated at different temperatures (initial fluoride concentration: 100 mg L^{-1}; dolomite dosage: 0.1 g; reaction time: 24 h; temperature: 25°C).

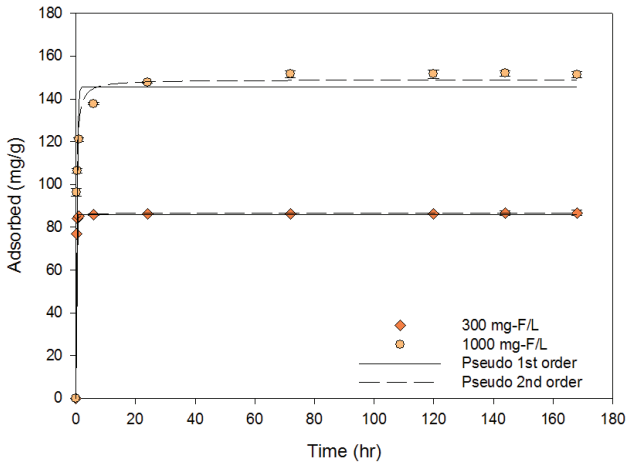

Fig. 4. Kinetic adsorption experiment data with model fittings of the pseudo-first-order and pseudo-second-order kinetic models for the adsorption of fluoride onto dolomite thermally treated at 800°C (initial fluoride concentration: 300 and 1,000 mg L^{-1}; adsorbent dosage: 0.1 g; reaction time: 0.25, 0.5, 1, 6, 24, 72, 120, 144, and 168 h; agitation speed: 100 rpm; temperature: 25°C).

3.2. Kinetic, equilibrium, and thermodynamic study of fluoride adsorption onto dolomite thermally treated at 800°C

Fluoride adsorption onto DTT-800 as a function of reaction time at two different fluoride concentrations (300 and 1,000 mg L^{-1}) is shown in Fig. 4, and the parameters for the pseudo-first-order and pseudo-second-order models are presented in Table 3. At a low initial concentration of fluoride (300 mg L^{-1}), fluoride adsorption reached equilibrium within 24 h, but 72 h duration was required to reach equilibrium for an initial fluoride concentration of 1,000 mg L^{-1}. The reaction rate constants of the pseudo-first-order and pseudo-second-order models for 300 mg L^{-1} were higher than those for 1,000 mg L^{-1}, indicating faster adsorption of fluoride onto DTT-800 at 300 mg L^{-1} than at 1,000 mg L^{-1}. The pseudo-second-order model (R^2 for 300 mg L^{-1}: 0.999; R^2 for 1000 mg L^{-1}: 0.955) described the observed data obtained at different reaction times better than the pseudo-first-order model (R^2 for 300 mg L^{-1}: 0.999; R^2 for 1,000 mg L^{-1}: 0.990), indicating that the adsorption rate of fluoride onto DTT-800 was primarily governed by chemisorption [23].

The relationships between the concentration of fluoride in aqueous phase and adsorbed fluoride onto DTT-800 at equilibrium are plotted in Fig. 5, and the parameters obtained from the Langmuir and Freundlich models are shown in Table 4. The higher R^2 value of the Freundlich model (R^2 = 0.988) compared with that of the Langmuir model (R^2 = 0.970) indicated that fluoride adsorption onto DTT-800 occurred via multiple layer adsorption rather than monolayer adsorption. The 1/*n* value of the Freundlich model was 0.26, which was less than 0.5, thereby indicating that the binding between fluoride and DTT-800 was strong [24]. The maximum fluoride adsorption capacity of DTT-800 obtained from the Langmuir model was 163.7 mg g^{-1}.

The maximum fluoride adsorption capacity of DTT-800 was comparable to that of other adsorbents published in the literature. Of the 102 adsorbents listed by Bhatnagar et al. [2], 99 had a lower fluoride adsorption capacity than the 163.7 mg g^{-1} capacity achieved in the current study. In three studies [9,11,24], the fluoride sorption capacity of the adsorbent was reported to be higher than that of DTT-800. However, the adsorption capacity of calcined Mg–Al–CO_3 layered double hydroxides [2] was not consistent with the maximum adsorption capacity of 141.64 mg g^{-1} reported by Lv et al. [25], which was less than that observed in this study. The fluoride adsorption capacities of Fe–Al–Ce trimetal oxide

Table 3
Kinetic model parameters obtained from model fitting of the experimental data at different reaction times

Initial fluoride concentration (mg L^{-1})	Pseudo-first-order kinetic model parameters			Pseudo-second-order kinetic model parameters		
	q_e (mg g^{-1})	k_1 (1/*h*)	R^2	q_e (mg g^{-1})	k_2 (g (mg·h)$^{-1}$)	R^2
300	85.99	8.93	0.999	86.60	0.43	0.999
1,000	148.73	3.21	0.955	148.96	0.04	0.990

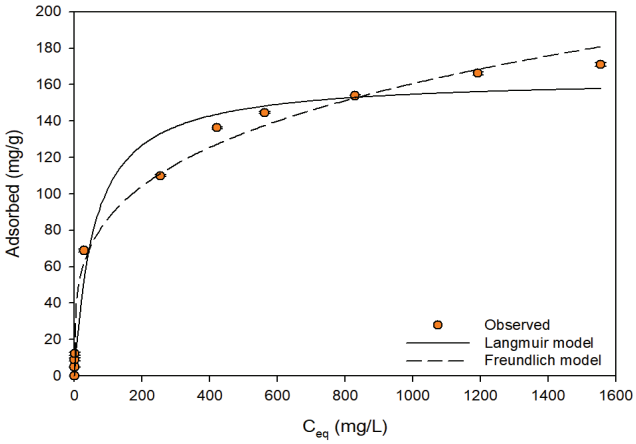

Fig. 5. Equilibrium adsorption experiment data with model fittings of the Langmuir and Freundlich isotherms for the adsorption of fluoride onto dolomite thermally treated at 800°C (initial fluoride concentration: 5, 10, 50, 100, 300, 500, 700, 1,000, 1,500, and 2000 mg L^{-1}; pH: 7.0; adsorbent dosage: 0.1 g; reaction time: 72 h; agitation speed: 100 rpm; temperature: 25°C).

Table 4
Equilibrium model parameters obtained from model fitting of the experimental data

Model	Parameters		R^2
Langmuir	Q_m (mg g^{-1})	K_L (L mg^{-1})	0.970
	163.7	58.4	
Freundlich	K_F ((mg F g^{-1})·(L mg^{-1} F)$^{1/n}$)	1/*n*	0.988
	25.2	0.26	

[9] and synthesized nanomagnesia (MgO nanoparticles) [11] were 178 and 267.82 mg g^{-1}, respectively. The base material of Fe–Al–Ce trimetal oxide, namely Ce, is an expensive rare earth metal, and the use of Ce is restricted for drinking water treatment [9]. Nanoparticles have a high adsorption capacity for fluoride due to their large specific surface area, but their toxicity restricts their use [26]. In addition to the limitations of toxicity, the synthesis of nanoparticles is also limited by cost and the difficulty to produce large quantities.

The thermodynamic parameters obtained from the thermodynamic analysis are provided in Table 5. As the temperature increased, the amount of fluoride adsorbed onto DTT-800 increased. The calculated $\Delta H°$ in this study was 32.79 kJ mol^{-1}. The positive $\Delta H°$ value indicated that the fluoride adsorption onto DTT-800 was endothermic. The $\Delta S°$ value was 109.38 J (K·mol)$^{-1}$, thereby indicating that the level of disorder increased at the solid-liquid interface during the

Table 5
Thermodynamic parameters for fluoride adsorption onto dolomite thermally treated at 800°C

Temperature (°C)	$\Delta H°$ (kJ mol^{-1})	$\Delta S°$ (J (K·mol)$^{-1}$)	$\Delta G°$ (kJ mol^{-1})
15	32.79	109.38	1.27
25			0.18
35			–0.92

adsorption process. As the temperature increased from 15°C to 35°C, the $\Delta G°$ values decreased gradually from 1.27 kJ mol^{-1} to –0.92 kJ mol^{-1}, thereby indicating that the adsorption reaction was prompted by the increasing temperature. The fluoride adsorption was spontaneous at 35°C but nonspontaneous at 15°C and 25°C.

3.3. Optimization studies by statistical experimental design for fluoride removal using dolomite thermally treated at 800°C

The Box-Behnken design of RSM was employed in this experiment to obtain a quadratic model consisting of 29 trials. The chosen range and levels of the four independent variables, namely solution pH, ionic strength, temperature, and reaction time, are shown in Table 1. *F*-value tests were performed using ANOVA to calculate the significance of the model employed in Design Expert statistical software. The results of Y_A recommended a quadratic model as the highest-order polynomial model that satisfied the criteria that any additional terms are significant and that the model is not aliased. The respective predicted responses were obtained as follows:

$$\begin{aligned} Y_A = {} & 153.55 - 10.77X_1 - 14.66X_2 + 24.03X_3 + 18.66X_4 \\ & + 6.79X_1X_2 - 0.49X_1X_3 - 0.082X_1X_4 - 0.87X_2X_3 \\ & - 4.07X_2X_4 + 1.15X_3X_4 - 9.29X_1^2 - 23.55X_2^2 - 55.65X_3^2 \\ & - 14.56X_4^2 \end{aligned} \quad (10)$$

The significance of the values of the model equation to determine the adsorption amount was checked by *F*, R^2, adjusted R^2, lack-of fit, and adequate precision tests. As shown in Table 6, the model *F*-value, which was calculated by dividing the mean square of each variable's effect by the mean square, was 35.94. The model probability value was <0.0001, which was less than 0.05, thereby indicating that the model terms for all calculated values were significant. The goodness-of-fit for each model was tested using the determination coefficient R^2, which was calculated to be 0.973. Its proximity to one indicated a good model fit to the observed

Table 6
Analysis of variance for the response surface methodology analysis of the amount of fluoride adsorbed onto a unit mass of dolomite thermally treated at 800°C (mg g^{-1})

Source	Sum of squares	*df*	Mean square	*F*-value	*p*-value Prob. > *F*
Model	37 384.04	14	2,670.2890	35.940	<0001
X_1	1,392.43	1	1,392.4300	18.740	.0007
X_2	2,578.74	1	2,578.7380	34.710	<0001
X_3	6,928.56	1	6,928.5620	93.250	<0001
X_4	4,178.64	1	4,178.6450	156.240	<0001
X_1X_2	184.17	1	184.1722	2.480	.1377
X_1X_3	0.95	1	0.9541	0.010	.9114
X_1X_4	0.03	1	0.0266	0.000	.9852
X_2X_3	3.02	1	3.0197	0.041	.8431
X_2X_4	66.16	1	66.1550	0.890	.3614
X_3X_4	5.33	1	5.3260	0.070	.7928
X_1^2	559.66	1	599.6638	7.530	.0158
X_2^2	3,596.15	1	3,596.1550	48.400	<0001
X_3^2	20 819.53	1	20 819.5300	280.220	<0001
X_4^2	1,374.76	1	1,374.7590	18.500	.0007
Residual	1,040.17	14	74.2979		
LoF	1,040.13	10	104.0132	10 556.550	<0001
PE	0.04	4	0.0099		
CT	38 424.21	28			

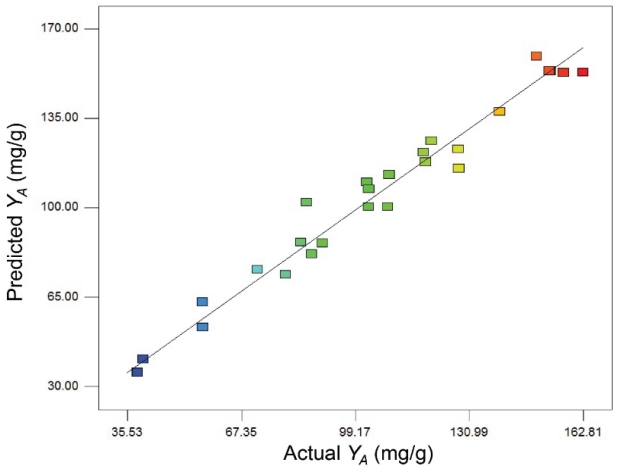

Fig. 6. Plot of predicted values vs. actual values for the amount of fluoride adsorbed onto a unit mass of dolomite thermally treated at 800°C (mg g^{-1}).

data. The adjusted R^2 value and the predicted R^2 value were 0.946 and 0.844, respectively. The adjusted and predicted R^2 values were in good agreement, and the adjusted R^2 values were close to each predicted R^2 value, thereby indicating a good adjustment between the observed and predicted values. The value of adequate precision, which reflects the signal-to-noise ratio, was 19.95, thereby indicating adequate signals with values greater than 4 [27]. The lack-of-fit tests used to evaluate the model adequacy indicated significant values for all responses, which reflected a poor fit. All the statistical results, except for the lack-of-fit tests, showed that the constructed model for removal percentage was suitable for describing the observed data. Fig. 6 shows that the points of the predicted versus actual plots for removal percentage were clustered along a diagonal line, thereby indicating that the predicted values matched well with the observed values.

The interactions of solution pH, ionic strength, temperature, and reaction time, which affected the removal percentage, were plotted as three-dimensional response surface curves against two experimental factors while the other factor was kept constant at its central value (Fig. 7). The regression model equation (Eq. (10)) determined the positive or negative influence of the variables on the amount of fluoride adsorption onto DTT-800. As shown in Table 6, both the first-order and second-order effects for all four variables on fluoride adsorption were significant (p <0.05), but the interaction effect of each pair of variables was not significant. The negative sign of the coefficients of X_1 and X_2 in the regression model equation indicated that fluoride removal by DTT-800 decreased with the increase in pH (from 4 to 8) and ionic strength (from 0 to 20 mM). In contrast to pH and ionic strength, temperature (15°C–35°C) and reaction time (36–72 h) positively influenced fluoride removal by DTT-800 as indicated by the positive sign of the coefficients of X_3 and X_4. The positive sign of X_3, namely reaction temperature, was also consistent with the results of the thermodynamic study, which showed that the fluoride adsorption onto DTT-800 was an endothermic reaction. The positive sign of X_4, namely reaction time, was consistent with the results of the kinetic study, which indicated that fluoride adsorption onto DTT-800 increased over the reaction time and reached equilibrium within 72 h. The coefficients of the square of each variable, i.e., X_1^2, X_2^2, X_3^2, and X_4^2, were negative, thereby indicating that the influence of each variable on fluoride adsorption was not constant. Such a result was also recognized from the curvature of each variable, as shown in Fig. 7.

pH and ionic strength, had a significant negative effect on fluoride adsorption onto DTT-800. The extent of fluoride adsorption onto Ca, Al, and Si oxides is strongly influenced by the pH of the solution because ligand exchange, which is the dominant mechanism of fluoride adsorption, involves the release of OH^- into solution [28,29]. Therefore, at high pH, the OH^- ion released from the adsorbent surface was inhibited, and less fluoride was adsorbed onto DTT-800. Yadav et al. [30] reported another explanation of this phenomenon: the competition of OH^- ions with fluoride for favorable adsorption sites (due to similarities in the charge and ionic radius these ions). In addition, increasing the pH leads to electrostatic repulsion between the negatively charged surface of DTT-800 and the anionic fluoride.

Fluoride adsorption onto DTT-800 was dependent on the ionic strength. Adsorption via inner-sphere complex formation is typically independent of ionic strength [31]. Since fluoride is removed by Ca-based adsorbents mainly by precipitation and chemisorption [2,32], the presence of an anion interferes with the fluoride adsorption onto DTT-800. Other researchers also observed the reduction in fluoride removal by the presence of anions owing to anionic competition for the adsorbent active sites. The impact of major anions on fluoride adsorption followed the order of HPO_4^{2-} > HCO_3^- >

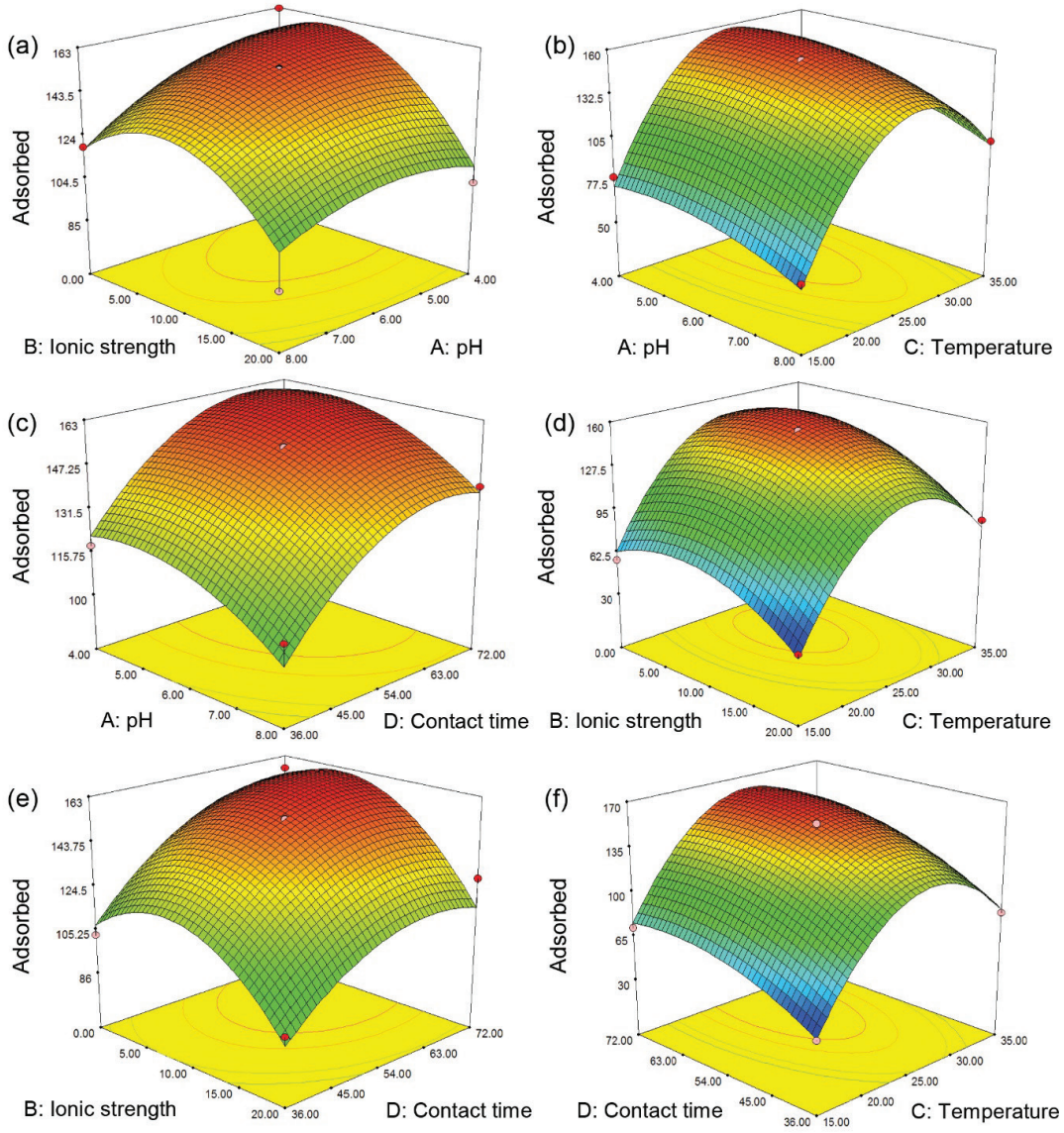

Fig. 7. Estimated response surface for the amount of fluoride adsorbed onto a unit mass of dolomite thermally treated at 800°C (mg g^{-1}) showing the effect of (a) pH and ionic strength, (b) pH and temperature, (c) pH and contact time, (d) ionic strength and temperature, (e) ionic strength and contact time, and (f) contact time and temperature.

SO_4^{2-} > Cl^- [33–35]. However, the influential pattern of these anions is not always consistent. Lv et al. [25] observed that fluoride removal in the presence of other ions decreased in the following order: PO_4^{3-} > Cl^- ≈ SO_4^{2-} > Br^- > > HCO_3^- > > NO_3^-. In addition to anion competition, water cluster formation on the surface of adsorbents at higher ionic strength can impede fluoride adsorption [36].

The optimal values of the variables, which maximized the amount of fluoride adsorbed onto a unit mass of DTT-800 (mg g^{-1}) (Y_A), was tracked using RSM. The highest Y_A, which was 165.91 mg g^{-1}, was obtained under a pH of 4.57, ionic strength of 7.45 mM, temperature of 28.30°C, and contact time of 58.33 h. The maximized response (165.91 mg g^{-1}) obtained from the RSM study was slightly higher than the maximum adsorption capacity of DTT-800 (163.7 mg g^{-1}) obtained from the equilibrium isotherm experiment.

3.4. Reuse of dolomite thermally treated at 800°C

Reutilization experiments were conducted to determine the amount of adsorbed fluoride and the number of times of use when DTT-800 was regenerated by washing it with distilled water. The amount of fluoride adsorption decreased from 118.8 to 25.0 mg g^{-1} as the number of times for the reuse of DTT-800 was increased, as shown in Fig. 8. According to these results, DTT-800 was not regenerated for fluoride removal by washing with deionized water. Although, better regeneration could be achieved via chemical or electrical regeneration processes, these chemicals and processes are too expensive to regenerate cheap adsorbents, i.e., DTT-800. The regeneration experiments also indicated that fluoride was strongly adsorbed to DTT-800. Only 5.8 mg g^{-1} was detached from DTT-800, to which 118.8 mg g^{-1} of fluoride

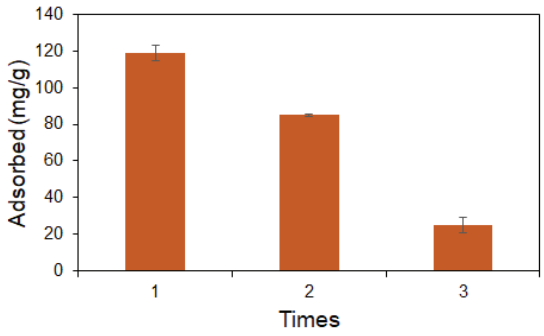

Fig. 8. Amount of fluoride removal for increasing cycles of reutilization (initial fluoride concentration: 1,000 mg L^{-1}; pH: 7.0; reaction time: 72 h; agitation speed: 100 rpm; temperature: 25°C).

was adsorbed (Cycle #1). Therefore, abandonment of DTT-800 after fluoride removal is recommended.

4. Conclusions

Dolomite was thermally treated to improve its fluoride adsorption capacity. The results showed that DTT-800 was more effective for fluoride removal than untreated dolomite and dolomite thermally treated at other temperatures. DTT-800 showed higher fluoride adsorption than DTT-900 because of its larger specific surface area and pore volume. The kinetic experiments showed that fluoride adsorption onto DTT-800 were mainly governed by chemisorption. The Freundlich model was more suitable for describing fluoride adsorption than the Langmuir model, indicating that fluoride was adsorbed onto DTT-800 via multi-layer adsorption. The maximum adsorption capacity of DTT-800 was 163.7 mg g^{-1}, which was superior to that of other adsorbents reported in the literature. Fluoride adsorption onto DTT-800 occurred via an endothermic reaction, which had an increased level of disorder at the solid-liquid interface. The effects of varying solution pH, ionic strength, reaction temperature, and time were examined, and the optimization of these parameters was accomplished using RSM. Solution pH and ionic strength had negative effects, but reaction temperature and time had positive effects on fluoride adsorption onto DTT-800. By applying the RSM model, the optimal experimental conditions maximized the parameters influencing fluoride removal. The results of the present investigation showed that thermal treatment is an easy but effective way to improve the adsorption capacity of dolomite. It can be concluded that thermally treated dolomite can be used as a low-cost, natural, and abundant adsorbent for the removal of fluoride from aqueous solution.

Acknowledgments

This work was supported by the Basic Science Research Program through the National Research Foundation of Korea funded by the Ministry of Education [grant number 2017R1D1A1B03030649].

References

[1] S.V. Jadhav, E. Bringas, G.D. Yadav, V.K.Rathod, I. Ortiz, K.V. Marathe, Arsenic and fluoride contaminated groundwaters: a review of current technologies for contaminants removal, J. Environ. Manage, 162 (2015) 306–325.
[2] A.Bhatnagar, E.Kumar, M. Sillanpää, Fluoride removal from water by adsorption—a review, Chem. Eng. J., 171 (2011) 811–840.
[3] P. Miretzky, A.F. Cirelli, Fluoride removal from water by chitosan derivatives and composites: a review, J. Fluorine. Chem., 132 (2011) 231–240.
[4] WHO. Guidelines for drinking water quality, Vol. 1–3. Geneva: World Health Organization Vol. 1–3 (1993) 45–46.
[5] M.A. Aboulhassan, S. Souabi, A. Yaacoubi, Pollution reduction and biodegradability index improvement of tannery effluents, Int. J. Environ. Sci. Technol., 5 (2008) 11–16.
[6] B.K. Shrivastava, A. Vani, Comparative study of defluoridation technologies in India, Asian J. Exp. Sci., 23 (2009) 269–274.
[7] S.J. Park, C.G. Lee, J.H. Kim, S.B. Kim, Y.Y. Chang, J.K. Yang, Bimetallic oxide-coated sand filter for simultaneous removal of bacteria, Fe(II), and Mn(II) in small-and pilot-scale column experiments, Desal. Wat. Treat, 54 (2015) 3380–3391.
[8] R. Bhaumik, N.K. Mondal, B. Das, P. Roy, K.C. Pal, C. Das, A. Baneerjee, Eggshell powder as an adsorbent for removal of fluoride from aqueous solution: equilibrium, kinetic and thermodynamic studies, J. Chem., 9 (2012) 1457–1480.
[9] X. Wu, Y. Zhang, X. Dou, M. Yang, Fluoride removal performance of a novel Fe–Al–Ce trimetal oxide adsorbent, Chemosphere, 69 (2007) 1758–1764.
[10] H. Liu, S. Deng, Z. Li, G. Yu, J. Huang, Preparation of Al-Ce hybrid adsorbent and its application for defluoridation of drinking water, J. Hazard. Mater., 179 (2010) 424–430.
[11] S.M. Maliyekkal, K.R. Antony, T. Pradeep, High yield combustion synthesis of nanomagnesia and its application for fluoride removal, Sci. Total Environ., 408 (2010) 2273–2282.
[12] K. Sasaki, M. Yoshida, B. Ahmmad, N. Fukumoto, T. Hirajima, Sorption of fluoride on partially calcined dolomite, Colloids. Surf. A., 435 (2013) 56–62.
[13] H. Roques, L. Nugroho-Jeudy, A. Lebugle, Phosphorus removal from wastewater by half-burned dolomite, Water Res., 25 (1991) 959–965.
[14] S.J. Park, H.K. An, Optimization of fabrication parameters for nanofibrous composite membrane using response surface methodology, Desal. Wat. Treat., 57 (2016) 20188–20198.
[15] D.C. Montgomery, Design and Analysis of Experiments, 5th ed., John Wiley & Sons, New York, 2001.
[16] R.H. Myers, D.C. Montgomery, Response Surface Methodology: Process and Product Optimization Using Designed Experiments, 2nd ed., John Wiley & Sons, New York, 2002.
[17] A.I. Rat'ko, A.I. Ivanets, A.I. Kulak, E.A. Morozov, I.O. Sakhar, Thermal decomposition of natural dolomite, Inorg. Mater., 47 (2011) 1372–1377.
[18] S. Gunasekaran, G. Anbalagan, Thermal decomposition of natural dolomite, Bull. Mater. Sci., 30 (2007) 339–344.
[19] K. Kang, C.G. Lee, J.W. Choi, S.G. Hong, S.J. Park, Application of thermally treated crushed concrete granules for the removal of phosphate: a cheap adsorbent with high adsorption capacity, Water Air Soil Pollut., 228 (2017) 8.
[20] H. Yin, X. Yan, X. Gu, Evaluation of thermally-modified calcium-rich attapulgite as a low-cost substrate for rapid phosphorus removal in constructed wetlands, Water Res., 115 (2017) 329–338.
[21] M.J. Kim, J.H. Lee, C.G. Lee, S.J. Park, Thermal treatment of attapulgite for phosphate removal: a cheap and natural adsorbent with high adsorption capacity, Desal. Wat. Treat., 114 (2018) 175–184.
[22] S. Karaca, A. Gürses, M. Ejder, M. Açıkyıldız, Adsorptive removal of phosphate from aqueous solutions using raw and calcinated dolomite, J. Hazard. Mater., 128 (2006) 273–279.
[23] E. Bulut, M. Özacar, I.A. Şengil, Equilibrium and kinetic data and process design for adsorption of Congo Red onto bentonite, J. Hazard. Mater., 154 (2008) 613–622.
[24] R.S. Summers, D.R.U. Knappe, V.L. Snoeyink, Adsorption of organic compounds by activated carbon. In: Water quality and treatment: A handbook on drinking water, 6th Edition, Edited by J. K. Edzwald. McGraw-Hill, 2011.

[25] L. Lv, J. He, M. Wei, X. Duan, Kinetic Studies on fluoride removal by calcined layered double hydroxides, Ind. Eng. Chem. Res., 45 (2006) 8623–8628.
[26] O. Bondarenko, K. Juganson, A. Ivask, K. Kasemets, M. Mortimer, A. Kahru, Toxicity of Ag, CuO and ZnO nanoparticles to selected environmentally relevant test organisms and mammalian cells in vitro: a critical review, Arch. Toxicol., 87 (2013) 1181–1200.
[27] S. Kamsonlian, B. Shukla, Optimization of process parameters using response surface methodology (RSM): removal of Cr (VI) from aqueous solution by wood apple shell activated carbon (WASAC), Res. J. Chem. Sci., 3 (2013) 31–37.
[28] M.B. McBride, Environmental soil chemistry. Oxford University Press. New York, 1994.
[29] E. Oguz, Adsorption of fluoride on gas concrete materials, J. Hazard. Mater., 117 (2005) 227–233.
[30] A.K. Yadav, C.P. Kaushik, A.K. Haritash, A. Kansal, N. Rani, Defluoridation of groundwater using brick powder as an adsorbent, J. Hazard. Mater., 128 (2006) 289–293.
[31] W. Stumm, J.J. Morgan, Aquatic Chemistry, 3rd ed., John Wiley & Sons, Inc. (1996) 533–549.
[32] M. Islam, R.K. Patel, Evaluation of removal efficiency of fluoride from aqueous solution using quick lime, J. Hazard. Mater., 143 (2007) 303–310.
[33] A. Tor, Y. Cengeloglu, M.E. Aydin, M. Ersoz, Removal of phenol from aqueous phase by using neutralized red mud, J. Colloid. Interface. Sci., 300 (2006) 498–503.
[34] Y. Tang, X. Guan, T. Su, N. Gao, J. Wang, Fluoride adsorption onto activated alumina: modeling the effects of pH and some competing ions, Colloids. Surf. A., 337 (2009) 33–38.
[35] Y. Tang, X. Guan, J. Wang, N. Gao, M.R. McPhail, C.C. Chusuei, Fluoride adsorption onto granular ferric hydroxide: effects of ionic strength, pH, surface loading, and major co-existing anions, J. Hazard. Mater., 171 (2009) 774–779.
[36] H.A. Arafat, M. Franz, N.G. Pinto, Effect of salt on the mechanism of adsorption of aromatics on activated carbon, Langmuir, 15 (1999) 5997–6003.